CHAPTER SIX

Use of Dynasore, the Small Molecule Inhibitor of Dynamin, in the Regulation of Endocytosis

Tom Kirchhausen,[*,1] Eric Macia,[*,‡] *and* Henry E. Pelish[*,†]

Contents

Abstract

The large GTPase dynamin is essential for clathrin-dependent coated-vesicle formation. Dynasore is a cell-permeable small molecule that inhibits the GTPase activity of dynamin1, dynamin2 and Drp1, the mitochondrial dynamin. Dynasore was discovered in a screen of ~16,000 compounds for inhibitors of

* Department of Cell Biology, Harvard Medical School, and IDI Immune Research Institute, Boston, Massachusetts
† Makoto Life Sciences, Inc., Boston, Massachusetts
‡ L'Institut de Pharmacologie Moléculaire et Cellulaire, CNRS, Valbonne, France
[1] Corresponding author

Methods in Enzymology, Volume 438
ISSN 0076-6879, DOI: 10.1016/S0076-6879(07)38006-3
© 2008 Elsevier Inc.
All rights reserved.

the dynamin2 GTPase. Dynasore is a noncompetitive inhibitor of dynamin GTPase activity and blocks dynamin-dependent endocytosis in cells, including neurons. It is fast acting (seconds) and its inhibitory effect in cells can be reversed by washout. Here we present a detailed synthesis protocol for dynasore, and describe a series of experiments used to analyze the inhibitory effects of dynasore on dynamin *in vitro* and to study the effects of dynasore on endocytosis in cells.

1. Introduction

Dynamin functions in membrane tubulation and fission of budding vesiculo-tubular structures. It is essential for clathrin-dependent endocytosis from the plasma membrane, for the fission of plasma membrane caveolae to form free transport vesicles, and for vesicle formation at the trans-Golgi network (Cao *et al.*, 2000; Corda *et al.*, 2002; Nichols, 2003; Takei *et al.*, 2005). It also appears to participate in actin comet formation and transport of macropinosomes and in the function of podosomes, probably by interaction with actin-binding proteins. A related role in membrane fission has also been assigned to homolog proteins of dynamin (Dnm1 in mammalian cells and Drp1 in yeast) in the biogenesis of mitochondria and peroxisomes (Koch *et al.*, 2005; Schrader, 2006).

2. Dynamin

Dynamin (for recent reviews, see Kirchhausen, 1999; Praefcke and McMahon, 2004; Thompson and McNiven, 2001; Wiejak and Wyroba, 2002; Yang and Cerione, 1999) is a multidomain protein of ~100 kDa containing a GTPase module, a lipid-binding pleckstrin homology (PH) domain, a GTPase effector domain (GED), and a proline/arginine-rich C-terminal segment (PRD) containing amino-acid sequences that bind to the SH3 domains of other proteins. Dynamin is unusual among GTPases because its affinity for GDP and GTP is rather low (10 to 25 μM) when compared to small and heterotrimeric GTPases, and because its intrinsic GTP hydrolysis rate is high (1 to 2 min^{-1}) and dramatically increases by polymerization (>100 min^{-1}) (referred to here as the intrinsic GAP activity). Because of its kinetic parameters and the high levels of intracellular GTP (1 mM), dynamin is thought to be only transiently in the GDP bound state (1 to 10 ms) (Sever *et al.*, 2000a). Pure dynamin spontaneously forms rings and spirals in conditions of low ionic strength, and decorates tubulin microtubules and lipid vesicles with helices of similar dimensions. Any condition leading to self-assembly or ring formation also leads to stimulation of the dynamin GTPase activity. A useful and simple trick to stimulate the

GTPase activity of dynamin is to mix it with GST-Grb2 (containing its two SH3 domains) (Barylko *et al.*, 1998). Using this approach, we screened for interfering small molecules and identified one compound that we named dynasore (Macia *et al.*, 2006). In cells, dynasore inhibits clathrin-mediated endocytosis at two distinct steps, the transition from a half-formed (''U'' pit) to fully formed pit and from a fully formed pit (''O'' pit) to an endocytic vesicle (Fig. 6.1).

There are several models to explain the role of dynamin in membrane tubulation and fission of budding vesiculotubular structures (reviewed in

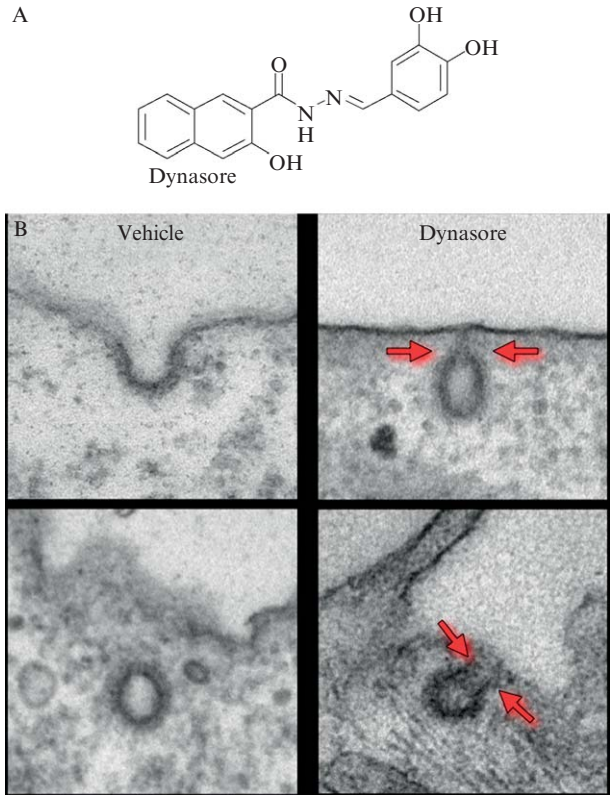

Figure 6.1 (A) Chemical structure of dynasore. (B) Effect of dynasore on clathrin-coated structures. The figure shows representative images of clathrin-coated structures of cells treated with DMSO (vehicle) or with 80 μM dynasore. The upper and lower left panels illustrate the appearance of endocytic coated pits and coated vesicles; the upper and lower right panels show the appearance of "U" and "O" shape-coated pits associated with the plasma membrane in cells treated with dynasore. The gray arrows highlight the extent of the constriction states observed upon treatment with dynasore. (From Macia, E., Ehrlich, M., Massol, R., Boucrot, E., Brunner, C., and Kirchhausen, T. (2006). Dynasore, a cell-permeable inhibitor of dynamin. *Dev. Cell* **10**, 839–850.)

Kelly, 1999; Kirchhausen, 1999; McNiven, 1998; Sever *et al.*, 2000b; Yang and Cerione, 1999). These models range from viewing dynamin strictly as a mechanochemical enzyme to considering it as a regulatory protein for the recruitment of the downstream enzymatic partner(s) responsible for fission. Viewed as a mechanochemical enzyme, dynamin self-assembles around the neck of the budding pit, and then undergoes a conformational change in response to GTP binding and/or GTP hydrolysis. It is assumed that the coordinated change in conformation of ring elements leads to neck constriction and scission, and many variants to this model have been proposed. These models are strongly influenced by the results from *in vitro* self-assembly studies, either alone or in the presence of flexible and inflexible lipid scaffolds (Stowell *et al.*, 1999; Sweitzer and Hinshaw, 1998; Zhang and Hinshaw, 2001). Dynamin viewed as a regulatory GTPase stems from studying the effects by overexpression of dynamin mutants defective in self-assembly and/or intrinsic GAP activity (Sever *et al.*, 1999). Based on the observation that dynR725A and dynK694A maintain or even stimulate the endocytic rate of receptor-mediated uptake of transferrin, it has been proposed that dynamin-GTP, rather than GTP hydrolysis, facilitates vesicle budding. The opposite view is held by McMahon and coworkers who analyzed the effect of overexpression of several point mutants of dynamin's GTPase effector (GED) and GTPase domains and found that dynamin oligomerization and GTP binding alone are not sufficient for endocytosis *in vivo*. They concluded that efficient GTP hydrolysis and an associated conformational change are also required (Marks *et al.*, 2001). When tested using microtubules or lipid tubes as assembly scaffolds, the intrinsic GAP activity of these mutants is about the same as with wildtype dynamin (Marks *et al.*, 2001; Sever *et al.*, 1999). Thus, it is possible that *in vivo*, the dynamin mutants assembled around membrane necks and displayed relatively "normal" GTPase activity.

3. Dynamin and the Actin Cytoskeleton

Dynamin, alone or in combination with amphiphysin, can form membrane tubes of dimensions similar to those on collars of deeply invaginated clathrin coated pits (Takei *et al.*, 1999). This was the first indication that a coated pit might not be a required template for dynamin function. Dynamin colocalizes with actin in growth cones (Torre *et al.*, 1994), and binds to a number of proteins involved in the regulation of actin cytoskeleton. They include profilin, cortactin, syndapin (a partner of N-WASP), and SH3-domain containing proteins like Abp1 linking cortical actin with endocytosis (Kessels *et al.*, 2001; McNiven *et al.*, 2000; Qualmann *et al.*, 1999; Witke *et al.*, 1998). Presently, it is not clear how these interactions are

in any way related to a possible link between actin and clathrin-based endocytosis, as suggested by the partial inhibition of receptor-mediated endocytosis induced on the depolymerization of actin with latrunculin or cytocholasin (Boucrot *et al.*, 2006). Dynamin is found in actin comets involved in intracellular movement of macropinosomes and of *Listeria* monocytogenes in infected cells (Lee and De Camilli, 2002; Orth *et al.*, 2002). It is also found in podosomes (Ochoa *et al.*, 2000), narrow membrane invaginations similar in diameter to the elongated necks of coated pits emanating from the plasma membrane; these membranes are surrounded by actin and are positioned perpendicular to the substratum. Overexpression of dynamin mutants defective in GTP binding and hydrolysis (dynK44A) or lacking the C-terminal PRD segment decreased the intracellular motility of macropinosomes and *Listeria* linked to actin comets (Lee and De Camilli, 2002; Orth *et al.*, 2002). It is not known whether the efficient linkage of dynamin and actin, or of its function in this context, requires dynamin assembly and intrinsic GAP activity.

4. The "Chemical Genetics" Discovery Approach

In the last decade, a number of laboratories have engaged in medium- and high-throughput phenotype-based screens of libraries of chemical compounds in an approach dubbed "chemical genetics." The stated goal is to identify small molecules that disrupt the function of proteins or protein complexes (Gura, 2000). The Institute of Chemistry and Cell Biology (ICCB) at Harvard Medical School, now the ICCB-Longwood, is a major screening center for this approach. Using its facilities, we have identified a compound, now called secramine, that blocks membrane traffic from the trans-Golgi network to the plasma membrane (Pelish *et al.*, 2001, 2006). A number of other compounds, such as Exo1, Exo2, BLT1, and vacuolin (Cerny *et al.*, 2004; Feng *et al.*, 2003, 2004; Nieland *et al.*, 2002), inhibit unique traffic steps along the secretory pathway or within endosomes. These small molecules were found by "forward chemical genetics," that is, use of a cell-based screen for inhibition or activation of a particular cellular process, followed by molecular target identification (Fig. 6.2). In the "reverse chemical genetics" approach, one first searches for compounds that inhibit or activate *in vitro* proteins known to be involved in a defined process, followed by studies to determine the phenotypic effects in cells and/or organisms. In comparison to "forward chemical genetics," this approach has the significant advantage of bypassing the target identification step, and was used for the discovery of dynasore (see Fig. 6.1A).

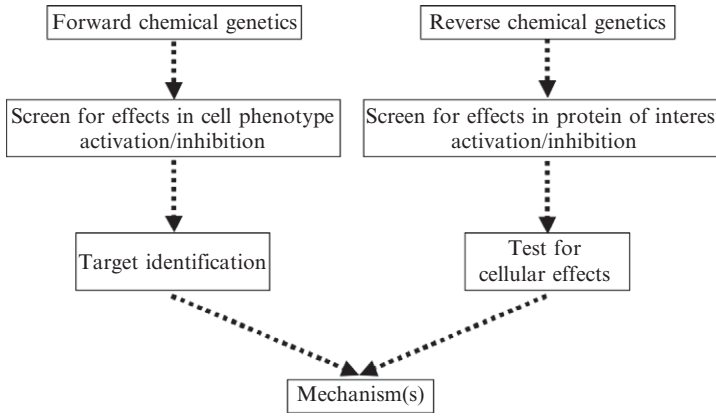

Figure 6.2 Strategy for the chemical genetics discovery approach. The reverse chemical genetics approach was used to discover dynasore. Dynasore is cell permeable and interferes with all functions known to be associated with dynamin. (From Macia, E., Ehrlich, M., Massol, R., Boucrot, E., Brunner, C., and Kirchhausen, T. (2006). Dynasore, a cell-permeable inhibitor of dynamin. *Dev. Cell* **10,** 839–850; and Newton, A. J., Kirchhausen, T., Murthy, V. N. (2006). Inhibition of dynamin completely blocks compensatory synaptic vesicle endocytosis. *Proc. Natl. Acad. Sci. USA* **103,** 17955–17960.)

5. Why Do We Need Interfering Small Molecules?

Interfering small molecules allow researchers to freeze biological processes at interesting points. This is particularly useful in the investigation of transient phenomena, such as membrane traffic. Much of the recent progress in understanding protein trafficking pathways has been achieved using approaches based on genetic dissection and morphological and biochemical analysis. However, the dynamic nature of these events (Cole *et al.*, 1996) makes it particularly difficult to use slow techniques such as genetic deletion and immunological depletion to study them. Temperature-sensitive (ts) mutants have in some cases proved helpful, but the number of proteins for which ts mutants exist is not large, and the effect can take several hours to be observable. Fast-acting chemical agents would be an ideal way to probe the dynamics of these complex systems.

5.1. Acute interference with membrane traffic

Only two ts mutants, one for dynamin and another for the ϵ-subunit of COPI, are available for studies in mammalian cells (Damke *et al.*, 1995; Guo *et al.*, 1994). The dynamin mutant displays an interfering phenotype within

minutes of transfer to the nonpermissive temperature, while the ϵ-mutant requires several hours before having a strong effect. Use of the dynamin ts mutant was instrumental in unraveling the enormous capacity of the endocytic pathway to accommodate perturbation. In less than 1 h after temperature shift, the rate of fluid phase uptake returns to normal levels (Damke *et al.*, 1995). This example illustrates the value of studying the effect of rapid perturbations in complex systems; the same can be said of studies involving the dramatic and acute effects of brefeldin A on the integrity of the Golgi complex, which led to our current views concerning the regulated traffic between the endoplasmic reticulum (ER) and the Golgi and the biogenesis of the Golgi (Pelletier *et al.*, 2000; Ward *et al.*, 2001). There are a few other chemicals that act in the endocytic and the secretory pathway, such as wortmanin (Kundra and Kornfeld, 1998; Spiro *et al.*, 1996), ilimaquinone (Takizawa *et al.*, 1993), and monensin (Pless and Wellner, 1996). Nevertheless, the chemical tools available are both few in number and unsatisfactory in terms of specificity for a particular protein target or cellular pathway. This deficiency exists because most of the available chemical tools were discovered serendipitously and not through directed screens. In addition to our directed screening approach, Robinson, McCluskey and coworkers screened for and identified a class of small molecules that inhibit the GTPase activity of dynamin1 *in vitro* (Hill *et al.*, 2005). The inhibitors they identified, dimeric tyrphostins, bear some resemblance to dynasore, as both display at least one benzenediol. Unlike dynasore, however, no *in vivo* data has been reported for these compounds.

6. Synthesis of Dynasore

We identified dynasore in a screen of ~16,000 compounds (part of the Diverset E, Chembridge Library) for inhibition of the GST-Grb2-stimulated GTPase activity of dynamin2 (Macia *et al.*, 2006) (assay described below). Here we describe our synthesis of dynasore (Fig. 6.3). Our approach is based on the strategy of Ling *et al.* (2001) for the synthesis of benzoic acid arylidenehydrazides. Dynasore ($C_{18}H_{14}N_2O_4$, molecular

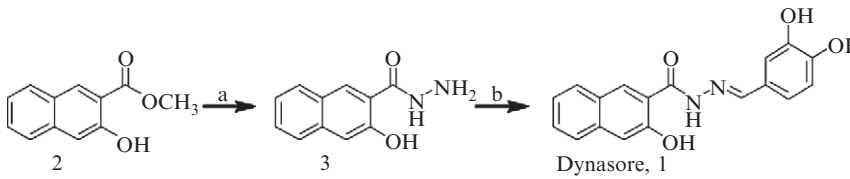

Figure 6.3 Scheme for the synthesis of dynasore. (a) H_4N_2, CH_3OH, 65°, 43% yield. (b) 3,4-dihydroxy-benzaldehyde, CH_3CO_2H, CH_3CH_2OH, 78°, 85% yield.

weight 322.31 g/mol) (1) is easily synthesized on gram scale in two steps from commercially available methyl 3-hydroxy-2-naphthoate (2) without the need for column chromatography.

Both reactions were performed in oven-dried glassware under a positive pressure of argon. Starting materials and reagents were purchased from commercial suppliers and used without further purification. ^{1}H and ^{13}C NMR spectra were recorded on a Varian INOVA500 or Mercury400 spectrometer. Chemical shifts for proton and carbon resonance are reported in parts per million (δ) relative to DMSO (δ 2.49 and 39.5, respectively). Tandem high-pressure liquid chromatography/mass spectral (LCMS) analyses were performed on a Waters Platform LCZ mass spectrometer in electrospray ionization (ES) mode. Samples were passed through a Symmetry C18 column using a gradient of 85% water/0.1% formic acid and 15% acetonitrile/0.1% formic acid to 100% acetonitrile/0.1% formic acid in 5 min.

The dynasore synthesis begins with the conversion of methyl 3-hydroxy-2-naphthoate (2) to 3-hydroxyl-2-naphtoylhydrazine (3). Hydrazine (2.3 ml, 5.0 equivalent) was added to a solution of methyl 3-hydroxy-2-naphthoate (2) (3 g, 14.8 mmol, 1.0 equivalent) in methanol (50 ml) at room temperature. The mixture was refluxed overnight at 65°. Upon cooling, brown needles formed. The solid was collected on a filter, washed with cold methanol, and dried to yield 3-hydroxyl-2-naphtoylhydrazine (3) (1.28 g, yield of 43%). The ^{1}H NMR (400 MHz, $(CD3)_2SO$) analysis follows: δ 8.44 (s, 1H), 7.81 (d, J = 8.0 Hz, ^{1}H) 7.71 (d, J = 8.1 Hz, ^{1}H), 7.45 to 7.49 (m, ^{1}H), 7.30 to 7.34 (m, ^{1}H), 7.26 (s, ^{1}H); 13C NMR (100 MHz, $(CD3)_2SO$): δ 167.0, 155.0, 135.8, 129.0, 128.6, 128.0, 126.6, 125.8, 123.6, 118.1, 110.6; and LCMS (ES+) calculated for $C_{11}H_{10}N_2O_2$ ($M\text{-}H^+$) was 203.07 (found 203.23).

We subsequently converted 3-hydroxyl-2-naphtoylhydrazine (3) into dynasore (3-hydroxy-naphthalene-2-carboxylic acid (3,4-dihydroxy-benzylidene)-hydrazide). Ethanol (50 ml) and acetic acid (0.4 ml) were added to 3 (1.28 g, 6.33 mmol, 1 equivalent) and 3,4-dihydroxy-benzaldehyde (0.87 g, 6.33 mmol, 1 equivalent). Upon heating to 78°, 3 and 3,4-dihydroxy-benzaldehyde dissolved. A new precipitate subsequently formed. The solution was refluxed overnight at 78°. Upon cooling, the precipitate was collected on a filter, washed with cold ethanol, and dried to yield pure dynasore (1.74 g, yield of 85%). The ^{1}H NMR (500 MHz, $(CD3)_2SO$) analysis follows: δ 11.80 (s, ^{1}H), 11.41 (s, ^{1}H), 9.44 (s, ^{1}H), 9.31 (s, ^{1}H), 9.29 (s, ^{1}H) 8.45 (s, ^{1}H), 8.24 (s, ^{1}H), 7.89 (d, J = 8.3 Hz, ^{1}H) 7.75 (d, J = 8.3 Hz, ^{1}H), 7.50 (dd, J = 7.6, 7.6 Hz, ^{1}H), 7.35 (dd, J = 7.6, 7.6, ^{1}H), 7.31 (s, ^{1}H), 7.28 (s, ^{1}H), 6.97 (d, J = 6.3 Hz); ^{13}C NMR (100 MHz, $(CD3)_2SO$): δ 163.6, 154.4, 149.2, 148.2, 145.8, 135.8, 130.0, 128.7, 126.8, 125.8, 125.5, 123.8, 120.9, 120.0, 115.6, 112.8, 110.6; and LCMS (ES+) calculated for $C_{18}H_{14}N_2O_4$ ($M\text{-}H^+$) was 323.10 (found 323.02).

7. Storage Conditions for Dynasore

Dynasore is stored as a dry solid under argon in the dark at –20°. Dynasore can also be stored at –20° or –80° in the dark (no need to flash freeze) as a 200-m*M* solution in DMSO under argon. Aliquots of 10 to 20 μl are stored in 0.5-ml microcentrifuge tubes. After adding argon and closing the cap, the microcentrifuge tubes are sealed with parafilm. To avoid the capture of moisture, the DMSO aliquots of dynasore are warmed up to room temperature before opening. The aqueous solution of dynasore will appear light yellow and the working final concentration for *in vivo* experiments is ~80 μM (0.2% DMSO final), which typically results in a greater than 90% block in endocytosis. An appropriate volume of the stock solution of dynasore is added to the working solution, and mixed by gentle tumbling or by up-and-down pipetting. Dynasore binds to serum proteins and loses activity. We thus use dynasore dissolved in media lacking albumin or serum. Typically we use DMEM ±10% Nuserum, PBS with glucose, or PBS with glucose and 10% Nuserum. Nuserum is a synthetic, low-protein alternative to traditional serum. For *in vivo* experiments, we first rinse the cells four to five times with serum-free medium (e.g., 3-ml sequential washes for cells seeded in a 12-well plate).

8. Expression, Purification, and Storage of Dynamin

8.1. Protein expression

We express human dynamin in SF9 insect cells (*Spodoptera frugiperda*, GIBCO-BRL, Gaithersburg, MD) grown in SF-900 II SFM (GIBCO-BRL) essentially as described (Damke *et al.*, 2001). Using the Bac-to-Bac baculovirus expression system (GIBCO-BRL), a full-length, cDNA encoding human dynamin1 containing a 6-His-tag at the N-terminus is subcloned into the baculovirus vector pFastBac. A bacmid is generated after transposition in *Escherichia coli*, and several independent clones are selected to transfect Sf9 cells using the transfection reagent CellFECTIN (Invitrogen, Carlsbad, CA).

For transfection, 10^6 SF9 cells are seeded in each well of a six-well plate containing 2 ml of Sf-900 II SFM medium supplemented with 0.5X penicillin/streptomycin. Prior to transfection, the cells are permitted to attach to the bottom of the plates for at least 1 h at 27°. Transfection proceeds as follows: (1) 5 μl of mini-prep bacmid (0.1 to 0.4 mg/ml) is added to 100μl of Sf 900 II SFM without antibiotics (solution A). (2) Separately, 6 μl

CellfFECTIN is added to 100 μl Sf-900 II SFM without antibiotics (solution B). (3) Solutions A and B are mixed and incubated at room temperature for 15 to 45 min. (4) The cells are washed once with 2 ml of Sf-900 II SFM without antibiotics. (5) Next, 0.8 ml of Sf-900 II SFM is added to each tube containing the lipid-DNA complexes, and then this solution is added to the cells. (6) After a 5-h incubation at 27°, the transfection mixtures are replaced with 2 ml of Sf-900 II SFM containing antibiotics, and the cells are incubated for 72 h at 27°. At this point, virus is harvested with the culture medium. We typically perform two extra rounds of virus amplification, by using a 1/100 dilution of the medium containing the virus. We dilute into 6 ml (round 1) and 20 ml (round 2) of Sf-900 II SFM containing penicillin/streptomycin in a 50-ml flask with 1×10^6 SF9 cells per milliliter. In each round, the cells are incubated for 72 h at 27°. A successful infection results in about 50% cell death, while the remaining cells are larger and contain granules easily observed by phase-contrast light microscopy. We normally verify protein expression levels at the end of the second round of virus amplification in SF9 cells using different dilutions of the virus stock (from 1/10 to 1/200 for 72 h at 27°; 106 SF9 cells seeded in a six-well plate containing 2 ml of Sf-900 II SFM supplemented with penicillin/streptomycin). We store the virus for up to 6 months in the dark at 4°.

For production of full-length dynamin, we infect 1 liter of Sf-900 II SFM media containing 1×10^6 SF9 cells per milliliter with a 1/1000 dilution of the amplified baculovirus stock. The cells are grown in a 2-liter spinner flask (80 rpm) for 72 h at 27°. Cells are then harvested by centrifugation (4000 rpm, 20 min, 4°) and stored at –20° until protein purification.

We constructed 6-His N-terminal–tagged human dynamin2ΔPRD (lacking the C-terminal, proline-rich domain) in a PET28a bacteria expression vector (Stratagene, La Jolla, CA). Using a Quickchange PCR mutagenesis protocol (Stratagene, La Jolla, CA), we introduced a stop codon at amino acid 747 (Warnock *et al.*, 1997). This recombinant protein is produced in *E. coli* BL21(DE3). In 2 to 4 liters of Luria-Bertani (LB) media, the bacteria are grown at 37° to an OD640, cooled to 18° in a water bath, subsequently induced with 0.25 mM IPTG, and further incubated overnight at 18°.

8.2. Protein purification and storage

N-terminal, His-tagged, full-length human dynamin1 and the truncated N-terminal, His-tagged human dynamin2 are purified using Ni-NTA and hydroxyapatite chromatography. All purification steps are carried out at 4°. Insect or bacteria cells are resuspended in 25 ml HCB250 containing protease inhibitor cocktail tablets (complete without EDTA, Boehringer Manheim, Indianapolis, IN) and cells disrupted by shearing using a laboratory model microfluidizer (Microfluidics, Newton MA). The lysates are then cleared by

centrifugation for 1 h at 40,000 rpm (Ti45 rotor, Beckman ultracentrifuge). The supernatants are added to a 2-ml 50% slurry of TALON beads (Clontech, Mountain View, CA). After gentle stirring for 4 h, the beads are loaded into a column and washed with 10 ml of HCB250 supplemented with 20 m*M* imidazole. Elution of the recombinant proteins (by gravity) then follows upon addition of 0.5 ml HCB250 containing 250 m*M* imidazole. The fractions containing dynamin are identified by 10% SDS-PAGE and Coomassie blue-staining. They are pooled and supplemented with a calpain inhibitor at 1 μM (Calbiochem, La Jolla, CA) and 5 m*M* $CaCl_2$. The inhibitor is essential at this point because a metalloprotease, probably activated by Ca^{2+}, seems to be activated during the next fractionation step. The sample is then loaded onto a 2-ml hydroxyapatite column (Bio-Scale^{TM} CHT2-I, 7 × 52 mm, Biorad, Hercules, CA) pre-equilibrated with 50 m*M* of K-PO_4 buffer. Bound proteins are eluted using a linear gradient from 50 to 500 m*M* of K-PO_4. The peak-containing fractions elute between 300 and 350 m*M* K-PO_4. Purified dynamin1 and dynamin2ΔPRD are stored at ~50 μM in 20% glycerol at –80° until use. Routinely we obtained about 2 mg/l of protein, of which the full-length constructs represent at least 90% of the total amount of protein. Prior to use, frozen aliquots (50 μl) are thawed rapidly to room temperature and centrifuged for 5 min at 14,000 rpm in a microfuge to remove any aggregated proteins.

9. Buffers and Reagents

Acid wash buffer: glycine 0.1 M, pH 2.5, and 150 m*M* NaCl

Penicillin/streptomycin solution: 1× corresponds to 100 units/ml of penicillin and 100 mg/ml of streptomycin

HEPES column buffer (HCB): 20 m*M* HEPES, pH 7, 2 m*M* EGTA, 1 m*M* $MgCl_2$, and 1 m*M* dithiothreitol (DTT)

HCB250: HCB supplemented with 250 m*M* NaCl

K-PO_4 hydroxyapatite buffer: 50 or 500 m*M*, pH 7.2, 1 m*M* DTT, and 1 μM calpain inhibitor

GTPase buffer: 10 m*M* Tris, pH 7.2, 2 m*M* $MgCl_2$, and 20 μM GTPγP32 (2000 dpm/pmol)

Acid-washed charcoal: 10% [w/v] activated charcoal (Sigma, St. Louis, MO) in an acidic solution of 2% (v/v) formic acid/8% (v/v) acetic acid

Malachite green solution: 0.324 m*M* malachite green, 0.0426% Triton X-100, 16.61 m*M* ammonium molybdate, and 1.246 M H_2SO_4. This solution is prepared fresh and used 2 h after; at this point the color of the solution becomes stable.

9.1. Colorimetric assay used during the screen for inhibitors of the stimulated GTPase activity of dynamin

This assay is based on the change of spectral characteristics of malachite green in the presence of free PO_4 ions (Cogan *et al.*, 1999; Maehama *et al.*, 2000). Independent of our work, a similar colorimetric assay was recently developed for studies with dynamin (Leonard *et al.*, 2005). The screen is initiated by mixing 100 n*M* of purified full-length human dynamin1 with 2 μM GST-Grb2 in a total volume of 30 μl containing 50 m*M* Tris, pH 7.5, 3 m*M* $MgCl_2$, 100 m*M* KCl, and 0.2 m*M* EGTA. Addition of GST-Grb2 (containing its two SH3 domains) stimulates full-length dynamin GTPase activity (Barylko *et al.*, 1998). We dispense this mixture into 384-well plates containing an optically clear bottom (Krackeler Scientific, Inc., Albany). A fresh malachite green solution is prepared on the day of use. After standing for ~2 h at room temperature, the color of the reagent changes from dark brown to golden yellow and is ready for use. On every plate, we use four columns as controls (DMSO without dynamin, GST-Grb2, or GTP). Approximately 100 nl of each compound (~10 m*M* dissolved in DMSO) is robotically pin-transferred to the assay plate, providing a final compound concentration range of 20 and 50 μM. The reaction is started by adding ~300 nl GTP (final concentration of 200 μM). After 30 min of incubation at room temperature, the reaction was terminated by the addition of 50 μl of malachite green solution. After 15 min at room temperature, the plates are placed on a plate reader (Perkin Elmer, Shelton, CT) and the absorbance is measured at 650 nm. We display and analyze the resulting data in Microsoft Office Excel (Microsoft, Redmond, WA) with the aid of a macro subroutine that facilitates the rapid identification of inhibitors in a given 384-well plate.

9.2. Radioactive assay for the GTPase activity of dynamin

This assay allows precise quantification of the dynasore activity and is a minor modification of the charcoal-based procedure described by Liu and colleagues (1996). We measure the GTPase activity of full-length dynamin1 or dynamin2 deleted of its PRD domain (dynamin2ΔPRD) at 0.2 μM, a concentration that minimizes spontaneous polymerization (Warnock *et al.*, 1997). The proteins are incubated at ambient temperature (~22°) in a final volume of 100 μl GTPase buffer for up to 30 min using solutions containing 20 or 150 m*M* NaCl for the low- or high-salt conditions, respectively. GTPase activity is terminated by transferring 10 μl of the reaction mixture into 500 μl of cold acid-washed charcoal (kept in ice in a 1.5-ml eppendorf tube), followed by centrifugation for 10 min (14,000 rpm in a microfuge at 4°). The amount of P32 released by hydrolysis, a measurement of GTP hydrolysis, is determined with a β-counter using 250 μl of the supernatant.

To identify dynasore as a noncompetitive inhibitor, we compared the Km and kcat values of the dynamin with the protein as an enzyme and GTP as a substrate. As shown in Fig. 6.4, the plot of the initial speed of the reaction (Vi) versus the concentration of GTP provides an estimate for Vmax (plateau) and Km (S concentration when Vi is half the Vmax). The Eadie-Hofstee linear transformation (V against V/[s]) can also be used for a more accurate representation; in this case the slope corresponds to –Km and the intercept on the x axis to V/Km.

9.3. Endocytic assay

Dynasore inhibits endocytosis in HeLa cells, human U373-MG astrocytes, COS-1 and BSC-1 cells (monkey cell lines), and mouse hippocampus neurons. In general, dynasore inhibition of endocytosis is measured at a cell density of 40 to 70%. Denser cultures are more resistant to the effects of dynasore.

One convenient way to detect the inhibitory effects of dynasore on endocytosis is to visually monitor its perturbation of the receptor-mediated uptake of transferrin. Transferrin receptors are constitutively internalized by a process that requires the formation of clathrin-coated pits and vesicles and is dynamin dependent (Ehrlich *et al.*, 2004; Hanover *et al.*, 1984). We normally follow the uptake of fluorescently tagged transferrin (e.g., Alexa-568 transferrin, Molecular Probes) at 37°. Before addition of transferrin, the

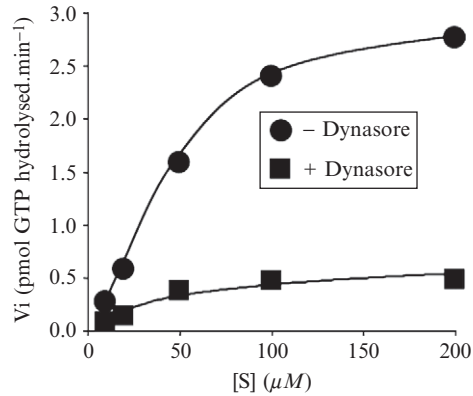

Figure 6.4 Determination of kinetics parameters for the effects of dynasore on the GTPase activity of dynamin. Effect of 40 μM dynasore on the rate of GTPase hydrolysis of 0.2 mM Dyn2ΔPRD determined at ambient temperature. The control experiment was done in the presence of 1% DMSO (vehicle) Initial rates of GTP hydrolysis were determined for different concentrations of GTP (S).

cells (between 40 and 70% confluency and grown on a coverslip) are incubated for 30 min at 37° with 80 μM dynasore or 0.2% DMSO only (vehicle control) in DMEM. In a pulse-chase format, we first allow binding of transferrin to its receptor at the surface of the cells after transfer at room temperature and incubation for 2 min (this step dramatically slows down endocytosis). After three washes with media (e.g., DMEM ± dynasore), cells are transferred to 37° and endocytosis proceeds. The receptor-bound Alexa-568 transferrin is internalized and transported first to peripherally located early endosomes (5 min) and then to the more perinuclear recycling/late endosomes (15 min). At different times, cells can be cooled to 4° (by addition of ice-chilled medium), followed by an acid wash (three consecutive 2-min washes each using 2 ml of acid wash buffer at room temperature under gentle agitation) to remove transferrin still bound at the cell surface. As the final step, the cells are fixed by incubation with a solution of PBS containing 4% PFA for 30 min at room temperature. Coverslips are then mounted on a glass slide, sealed with nail polish and are ready for fluorescence microscopy.

We acquire images using a spinning disk confocal head (Perkin Elmer) attached to an inverted microscope (200M, Zeiss Co.) under control of Slide Book 4 (Intelligent Imaging Innovations, Inc.) as described (Ehrlich *et al.*, 2004). For each cell, we acquired a series of confocal sections imaged every 0.3 μm. The integrated projected fluorescence of 80 to 100 cells is analyzed for each condition (dynasore concentration or time kinetics). To normalize between images, we set the fluorescence intensity of the vehicle control at 100%.

In the above experiment, we observed a strong block in the traffic and accumulation of transferrin with 80 μM dynasore. This inhibition is dose dependent with an IC50 ($\sim$15 μM). The decrease in transferrin uptake is not due to a decrease in the number of transferrin receptors at the cell surface or to a decrease in the association of transferrin with its receptor, as the amount of surface-bound transferrin is the same in cells kept for 30 min at 4° in the presence of dynasore or vehicle control.

Other assays, which are beyond the scope of this paper, are useful for following the effect of dynasore on the endocytosis of other ligands such as LDL, viruses, and bacteria.

ACKNOWLEDGMENT

We thank Matthew D. Shair for use of his laboratory facilities to carry out the synthesis of dynasore. We also thank members of the Kirchhausen lab who participated in the discovery and characterization of dynasore activity, including Chris Brunner, Marcelo Erlich, Ramiro Massol, Werner Boll, and Emmanuel Boucrot. We acknowledge support from the National Institutes of Health (grants GM GM62566, GM03548, and GM075252 to T. K.).

REFERENCES

Barylko, B., Binns, D., Lin, K. M., Atkinson, M. A. L., Jameson, D. M., Yin, H. L., and Albanesi, J. P. (1998). Synergistic activation of dynamin gtpase by grb2 and phosphoinositides. *J. Biol. Chem.* **273,** 3791–3797.

Boucrot, E., Saffarian, S., Massol, R., Kirchhausen, T., and Ehrlich, M. (2006). Role of lipids and actin in the formation of clathrin-coated pits. *Exp. Cell Res.* **312,** 4036–4048 (Epub 2006 Sep 4030.).

Cao, H., Thompson, H. M., Krueger, E. W., and McNiven, M. A. (2000). Disruption of Golgi structure and function in mammalian cells expressing a mutant dynamin. *J. Cell Sci.* **113,** 1993–2002.

Cerny, J., Feng, Y., Yu, A., Miyake, K., Borgonovo, B., Klumperman, J., Meldolesi, J., McNeil, P. L., and Kirchhausen, T. (2004). The small chemical vacuolin-1 inhibits $Ca^{(2+)}$-dependent lysosomal exocytosis but not cell resealing. *EMBO Rep.* **5,** 883–888.

Cogan, E. B., Birrell, G. B., and Griffith, O. H. (1999). A robotics-based automated assay for inorganic and organic phosphates. *Anal. Biochem.* **271,** 29–35.

Cole, N. B., Smith, C. L., Sciaky, N., Terasaki, M., Edidin, M., and Lippincott-Schwartz, J. (1996). Diffusional mobility of Golgi proteins in membranes of living cells. *Science* **273,** 797–800.

Corda, D., Hidalgo Carcedo, C., Bonazzi, M., Luini, A., and Spano, S. (2002). Molecular aspects of membrane fission in the secretory pathway. *Cell. Mol. Life Sci.* **59,** 1819–1832.

Damke, H., Baba, T., Vanderbliek, A. M., and Schmid, S. L. (1995). Clathrin-independent pinocytosis is induced in cells overexpressing a temperature-sensitive mutant of dynamin. *J. Cell Biol.* **131,** 69–80.

Damke, H., Muhlberg, A. B., Sever, S., Sholly, S., Warnock, D. E., and Schmid, S. L. (2001). Expression, purification, and functional assays for self association of dynamin-1. *Methods Enzymol.* **329,** 447–457.

Ehrlich, M., Boll, W., Van Oijen, A., Hariharan, R., Chandran, K., Nibert, M. L., and Kirchhausen, T. (2004). Endocytosis by random initiation and stabilization of clathrin-coated pits. *Cell* **118,** 591–605.

Feng, Y., Yu, S., Lasell, T. K. R., Jadhav, A. P., Macia, E., Chardin, P., Melancon, P., Roth, M., Mitchison, T., and Kirchhausen, T. (2003). Exo1: A new chemical inhibitor of the exocytic pathway. *Proc. Natl. Acad. Sci. USA* **100,** 6469–6474.

Feng, Y., Jadhav, A. P., Rodighiero, C., Fujinaga, Y., Kirchhausen, T., and Lencer, W. I. (2004). Retrograde transport of cholera toxin from the plasma membrane to the endoplasmic reticulum requires the trans-Golgi network but not the Golgi apparatus in Exo2-treated cells. *EMBO Rep.* **5,** 596–601.

Guo, Q., Vasile, E., and Krieger, M. (1994). Disruptions in Golgi structure and membrane traffic in a conditional lethal mammalian cell mutant are corrected by epsilon-COP. *J. Cell Biol.* **125,** 1213–1224.

Gura, T. (2000). A chemistry set for life. *Nature* **407,** 282–284.

Hanover, J. A., Willingham, M. C., and Pastan, I. (1984). Kinetics of transit of transferrin and epidermal growth factor through clathrin-coated membranes. *Cell* **39,** 283–293.

Hill, T., Odell, L. R., Edwards, J. K., Graham, M. E., McGeachie, A. B., Rusak, J., Quan, A., Abagyan, R., Scott, J. L., Robinson, P. J., and McCluskey, A. (2005). Small molecule inhibitors of dynamin I GTPase activity: development of dimeric tyrphostins. *J. Med. Chem.* **48,** 7781–7788.

Kelly, R. B. (1999). New twists for dynamin. *Nat. Cell Biol.* **1,** E8–E9.

Kessels, M. M., Engqvist-Goldstein, A. E. Y., Drubin, D. G., and Qualmann, B. (2001). Mammalian Abp1, a signal-responsive F-actin-binding protein, links the actin cytoskeleton to endocytosis via the GTPase dynamin. *J. Cell Biol.* **153,** 351–366.

Kirchhausen, T. (1999). Cell biology—Boa constrictor or rattlesnake? *Nature* **398,** 470–471.

Koch, A., Yoon, Y., Bonekamp, N. A., McNiven, M. A., and Schrader, M. (2005). A role for Fis1 in both mitochondrial and peroxisomal fission in mammalian cells. *Mol. Biol. Cell* **16,** 5077–5086. (Epub 2005 Aug 5017.)

Kundra, R., and Kornfeld, S. (1998). Wortmannin retards the movement of the mannose 6-phosphate/insulin-like growth factor II receptor and its ligand out of endosomes. *J. Biol. Chem.* **273,** 3848–3853.

Lee, E., and De Camilli, P. (2002). Dynamin at actin tails. *Proc. Natl. Acad. Sci. USA* **99,** 161–166.

Leonard, M., Song, B. D., Ramachandran, R., and Schmid, S. L. (2005). Robust colorimetric assays for dynamin's basal and stimulated GTPase activities. *Methods Enzymol.* **404,** 490–503.

Ling, A., Hong, Y., Gonzalez, J., Gregor, V., Polinsky, A., Kuki, A., Shi, S., Teston, K., Murphy, D., Porter, J., Kiel, D., Lakis, J., *et al.* (2001). Identification of alkylidene hydrazides as glucagon receptor antagonists. *J. Med. Chem.* **44,** 3141–3149.

Liu, J. P., Zhang, Q. X., Baldwin, G., and Robinson, P. J. (1996). Calcium binds dynamin I and inhibits its GTPase activity. *J. Neurochem.* **66,** 2074–2081.

Macia, E., Ehrlich, M., Massol, R., Boucrot, E., Brunner, C., and Kirchhausen, T. (2006). Dynasore, a cell-permeable inhibitor of dynamin. *Dev. Cell* **10,** 839–850.

Maehama, T., Taylor, G. S., Slama, J. T., and Dixon, J. E. (2000). A sensitive assay for phosphoinositide phosphatases. *Anal. Biochem.* **279,** 248–250.

Marks, B., Stowell, M. H. B., Vallis, Y., Mills, I. G., Gibson, A., Hopkins, C. R., and McMahon, H. T. (2001). GTPase activity of dynamin and resulting conformation change are essential for endocytosis. *Nature* **410,** 231–235.

McNiven, M. A. (1998). Dynamin: a molecular motor with pinchase action. *Cell* **94,** 151–154.

McNiven, M. A., Kim, L., Krueger, E. W., Orth, J. D., Cao, H., and Wong, T. W. (2000). Regulated interactions between dynamin and the actin-binding protein cortactin modulate cell shape. *J. Cell Biol.* **151,** 187–198.

Newton, A. J., Kirchhausen, T., and Murthy, V. N. (2006). Inhibition of dynamin completely blocks compensatory synaptic vesicle endocytosis. *Proc. Natl. Acad. Sci. USA* **103,** 17955–17960.

Nichols, B. (2003). Caveosomes and endocytosis of lipid rafts. *J. Cell Sci.* **116,** 4707–4714.

Nieland, T. J. F., Penman, M., Dori, L., Krieger, M., and Kirchhausen, T. (2002). Discovery of chemical inhibitors of the selective transfer of lipids mediated by the HDL receptor SR-BI. *Proc. Natl. Acad. Sci. USA* **99,** 15422–15427.

Ochoa, G. C., Slepnev, V. I., Neff, L., Ringstad, N., Takei, K., Daniell, L., Kim, W., Cao, H., McNiven, M., Baron, R., and De Camilli, P. (2000). A functional link between dynamin and the actin cytoskeleton at podosomes. *J. Cell Biol.* **150,** 377–389.

Orth, J. D., Krueger, E. W., Cao, H., and McNiven, M. A. (2002). The large GTPase dynamin regulates actin comet formation and movement in living cells. *Proc. Natl. Acad. Sci. USA* **99,** 167–172.

Pelish, H. E., Westwood, N. J., Feng, Y., Kirchhausen, T., and Shair, M. D. (2001). Use of biomimetic diversity-oriented synthesis to discover galanthamine-like molecules with biological properties beyond those of the natural product. *J. Am. Chem. Soc.* **123,** 6740–6741.

Pelish, H. E., Peterson, J. R., Salvarezza, S. B., Rodriguez-Boulan, E., Chen, J. L., Stamnes, M., Macia, E., Feng, Y., Shair, M. D., and Kirchhausen, T. (2006). Secramine inhibits Cdc42-dependent functions in cells and Cdc42 activation *in vitro*. *Nat. Chem. Biol.* **2,** 39–46.

Pelletier, L., Jokitalo, E., and Warren, G. (2000). The effect of Golgi depletion on exocytic transport. *Nat. Cell Biol.* **2,** 840–846.

Pless, D. D., and Wellner, R. B. (1996). In vitro fusion of endocytic vesicles: effects of reagents that alter endosomal pH. *J. Cell. Biochem.* **62,** 27–39.

Praefcke, G. J., and McMahon, H. T. (2004). The dynamin superfamily: universal membrane tubulation and fission molecules? *Nat. Rev. Mol. Cell Biol.* **5,** 133–147.

Qualmann, B., Roos, J., DiGregorio, P. J., and Kelly, R. B. (1999). Syndapin I, a synaptic dynamin-binding protein that associates with the neural Wiskott–Aldrich syndrome protein. *Mol. Biol. Cell* **10,** 501–513.

Schrader, M. (2006). Shared components of mitochondrial and peroxisomal division. *Biochim. Biophys. Acta* **1763,** 531–541. (Epub 2006 Feb 2002.)

Sever, S., Muhlberg, A. B., and Schmid, S. L. (1999). Impairment of dynamin's GAP domain stimulates receptor-mediated endocytosis. *Nature* **398,** 481–486.

Sever, S., Damke, H., and Schmid, S. L. (2000a). Dynamin:GTP controls the formation of constricted coated pits, the rate limiting step in clathrin-mediated endocytosis. *J. Cell Biol.* **150,** 1137–1148.

Sever, S., Damke, H., and Schmmid, S. L. (2000b). Garrotes, springs, ratches and whips: putting dynamin models to test. *Traffic* **1,** 385–392.

Spiro, D. J., Boll, W., Kirchhausen, T., and Wessling-Resnick, M. (1996). Wortmannin alters the transferrin receptor endocytic pathway *in vivo* and *in vitro*. *Mol. Biol. Cell* **7,** 355–367.

Stowell, M. H. B., Marks, B., Wigge, P., and McMahon, H. T. (1999). Nucleotide-dependent conformational changes in dynamin: Evidence for a mechanochemical molecular spring. *Nat. Cell Biol.* **1,** 27–32.

Sweitzer, S. M., and Hinshaw, J. E. (1998). Dynamin undergoes a GTP-dependent conformational change causing vesiculation. *Cell* **93,** 1021–1029.

Takei, K., Slepnev, V. I., Haucke, V., and de Camilli, P. (1999). Functional partnership between amphiphysin and dynamin in clathrin-mediated endocytosis. *Nat. Cell. Biol.* **1,** 33–39.

Takei, K., Yoshida, Y., and Yamada, H. (2005). Regulatory mechanisms of dynamin-dependent endocytosis. *J. Biochem. (Tokyo)* **137,** 243–247.

Takizawa, P. A., Yucel, J. K., Veit, B., Faulkner, D. J., Deerinck, T., Soto, G., Ellisman, M., and Malhotra, V. (1993). Complete vesiculation of Golgi membranes and inhibition of protein transport by a novel sea sponge metabolite, ilimaquinone. *Cell* **73,** 1079–1090.

Thompson, H. M., and McNiven, M. A. (2001). Dynamin: switch or pinchase? *Curr. Biol.* **11,** R850.

Torre, E., McNiven, M. A., and Urrutia, R. (1994). Dynamin 1 antisense oligonucleotide treatment prevents neurite formation in cultured hippocampal neurons. *J. Biol. Chem.* **269,** 32411–32417.

Ward, T. H., Polishchuk, R. S., Caplan, S., Hirschberg, K., and Lippincott-Schwartz, J. (2001). Maintenance of Golgi structure and function depends on the integrity of ER export. *J. Cell Biol.* **155,** 557–570. (Epub 2001 Nov 2012.)

Warnock, D. E., Baba, T., and Schmid, S. L. (1997). Ubiquitously expressed dynamin-II has a higher intrinsic GTPase activity and a greater propensity for self-assembly than neuronal dynamin-I. *Mol. Biol. Cell* **8,** 2553–2562.

Wiejak, J., and Wyroba, E. (2002). Dynamin: characteristics, mechanism of action and function. *Cell. Mol. Biol. Lett.* **7,** 1073–1080.

Witke, W., Podtelejnikov, A. V., Dinardo, A., Sutherland, J. D., Gurniak, C. B., Dotti, C., and Mann, M. (1998). In mouse brain profilin I and profilin II associate with regulators of the endocytic pathway and actin assembly. *EMBO J.* **17,** 967–976.

Yang, W. N., and Cerione, R. A. (1999). Endocytosis: Is dynamin a 'blue collar' or 'white collar' worker? *Curr. Biol.* **9,** R511–R514.

Zhang, P. J., and Hinshaw, J. E. (2001). Three-dimensional reconstruction of dynamin in the constricted state. *Nat. Cell Biol.* **3,** 922–926.